Climatic variability during the last millennium in Western Iceland from lake sediment records

HOLMES, Naomi <http://orcid.org/0000-0002-0665-3518>, LANGDON, Peter G., CASELDINE, Chris J., WASTEGARD, Stefan, LENG, Melanie J., CROUDACE, Ian W. and DAVIES, Siwan M.

Published version

HOLMES, Naomi, LANGDON, Peter G., CASELDINE, Chris J., WASTEGARD, Stefan, LENG, Melanie J., CROUDACE, Ian W. and DAVIES, Siwan M. (2016). Climatic variability during the last millennium in Western Iceland from lake sediment records. The Holocene, 26 (5), 756-771.

Climatic variability during the last millennium in Western Iceland from lake sediment records

Naomi Holmes[a], Peter G. Langdon[b*], Chris J. Caseldine[c], Stefan Wastegård[d], Melanie J. Leng[e,f], Ian W. Croudace[g] and Siwan M. Davies[h]

[a]Department of the Natural and Built Environment, Sheffield Hallam University, Sheffield, S1 1WB, UK

[b]Geography and Environment, University of Southampton, Southampton, SO17 1BJ, UK

[c]Geography, Penryn Campus, University of Exeter, Penryn, Cornwall, TR10 9FE, UK

[d]Department of Physical Geography, Stockholm University, SE-106 91 Stockholm, Sweden

[e]Centre for Environmental Geochemistry, School of Geography, University of Nottingham, Nottingham, NG7 2RD, UK

[f]NERC Isotope Geosciences Facilities, British Geological Survey, Keyworth, Nottingham, NG12 5GG, UK

[g]Ocean and Earth Science, University of Southampton, National Oceanography Centre Southampton, European Way, Southampton, SO14 3ZH, UK

[h]Department of Geography, College of Science, Swansea University, Singleton Park, Swansea, SA2 8PP, UK

*Corresponding author

Abstract

The aim of this research was to create a decadal scale terrestrial quantitative palaeoclimate record for NW Iceland from lake sediments for the last millennium. Geochemical, stable isotope and chironomid reconstructions were obtained from a lake sequence constrained by tephra deposits on the Snæfellsnes peninsula, W Iceland. Obtaining a quantitative record proved problematic, but the qualitative chironomid record showed clear trends associated with past summer temperatures, and the sedimentological records provided evidence for past changes in precipitation, mediated through catchment soil inwash. When the full range of chronological uncertainty is considered, four clear phases of climatic conditions were identified: (1) a relatively warm phase between AD 1020 - 1310; (2) a relatively stable period between AD 1310 and AD 1510, cooler than the preceding period, but still notably warmer that the second half of the millennium; (3) a consistent reduction of temperatures between AD 1560 - 1810, with the coolest period between AD 1680-1810; (4) AD 1840 - 2000 has temperatures mainly warmer than in the preceding two centuries, with a rising trend and increased variability from c. AD 1900 onwards. The reconstructions show clearly that the first half of the millennium experienced warmer climatic conditions than the second half, with a return to the warmer climate only occurring in the last c. 100 years. Much of the variability of the chironomid record can be linked to changes in the North Atlantic Oscillation (NAO). The reconstructions presented can track low frequency and long-term trends effectively and consistently but high resolution and calibrated quantitative records remain more of a challenge – not just in finding optimal sedimentary deposits, but also in finding the most reliable proxy. It is this that presents the real challenge for Holocene climate reconstruction from this key area of the North Atlantic.

Keywords

Iceland – palaeolimnology – chironomids– Little Ice Age – Medieval Climate Anomaly – North Atlantic Oscillation

57 **Introduction**

58 Understanding spatial variability in palaeoclimatic reconstruction relies heavily on high resolution
59 quantitative data provided from climate proxies. Because of the importance of the sensitivity of the
60 arctic and sub-arctic to climate change there have been attempts to derive such reconstructions for
61 the North Atlantic (Kaufman et al., 2009) and a number of sites in Iceland have been examined for
62 their palaeolimnological records to potentially be used for such reconstructions (Axford et al., 2009;
63 2011; Geirsdóttir et al., 2009a; Langdon et al., 2011; Larsen et al., 2011, 2012). Typically it has
64 proved problematic to calibrate Icelandic proxy records into a quantitative temperature record. For
65 example a biogenic silica (BSi) record for the last 2000 years from the Icelandic site Haukadalsvatn
66 has been shown to be a proxy for spring/summer conditions related to diatom productivity
67 (Geirsdóttir et al., 2009b), but it did not prove possible to calibrate this quantitatively. At other lakes
68 in Iceland attempts have been made to provide quantitative data utilising chironomid-inferred July
69 temperatures based on the Icelandic chironomid training set (Axford et al., 2007; Langdon et al.,
70 2008, Holmes et al., 2011), and a multi-decadal scale summer temperature record now exists for NW
71 Iceland since AD 1650 (Langdon et al., 2011). Longer records do exist, but at lower resolution
72 (centennial scale) and quantification has relied on DCA axis related temperature correlations (Axford
73 et al., 2009) or using a Norwegian chironomid training set (Caseldine et al., 2003).
74 Palaeolimnological approaches have therefore yet to provide consistent high-resolution quantitative
75 terrestrial temperature records for the later Holocene in Iceland. There are a number of potential
76 reasons for this:

77 (1) It is still unclear what sort of lake provides the best sediments for analysis in Iceland. Axford
78 et al. (2009) have highlighted difficulties with large, deep lakes, especially for chironomid
79 based temperature reconstruction approaches. Additionally, with any transfer function
80 approach, there may be problems associated with secondary gradients (Juggins 2013), and
81 hence caution is required in interpreting such reconstructions;
82 (2) Altitude may also be significant as the only Icelandic lake to produce chironomid based proxy
83 results that correlate well with instrumental data, Mýfluguvatn, lies at 435 m above sea level
84 (Langdon et al., 2011), and may well indicate that it is only at higher altitudes that climate
85 changes will be significant enough to register in the faunal or sedimentary records. If this is
86 the case then these lakes are likely to have relatively low sedimentation rates, and relatively
87 low concentrations of potential proxies;
88 (3) Post Settlement (~AD 874) human influences on catchments, particularly soil erosion
89 (McGovern et al., 2007), have been shown to affect chironomid assemblages within lakes

(Lawson et al., 2007). Careful site selection, limiting the effects of human settlements, is important, particularly over the instrumental (calibration) period;

(4) There are as yet few proxies that have the potential to provide quantitative palaeoclimatic data. % BSi has been interpreted as responding to local diatom productivity, which in turn is a function of climate, especially the duration of the ice-free season and spring temperatures (Geirsdóttir et al., 2009b; Striberger et al., 2012), but does not yet provide a quantitative signal. Similarly at Haukadalsvatn Geirsdóttir et al. (2009b) have shown that the sediment total organic carbon content (TOC) is strongly related to soil erosion and summer temperatures, but again not yet quantified. Chironomid-based calibration models can be used to provide chironomid-inferred temperature (C-IT) reconstructions (Langdon et al., 2008; Axford et al., 2007, 2009; Holmes et al., 2011) although they have not yet been widely tested at a variety of locations and lake types in Iceland;

(5) Chronology and sedimentation rate still play an important role in determining whether lake sediments can provide high resolution, robust data. Radiocarbon dating has been found to present problems in Iceland (Geirsdóttir et al., 2009b), ideally requiring a sound tephrochronology for age-depth profiles, possibly with assistance from palaeomagnetism (Ólafsdóttir et al., 2013).

Multiproxy, tephrochronologically constrained data presented here from Baulárvallavatn, studied as part of the EU-funded MILLENNIUM project, attempt to address the issues raised above. Owing to the location of Iceland in such an important position for the climate of the North Atlantic and the development of high quality marine records that are now available for the region (e.g., Massé et al., 2008; Ólafsdóttir et al., 2010; Sicre et al., 2011; Cunningham et al. 2013) it is important to determine how best to provide the necessary terrestrial equivalent and the results from this study reveal both the potential and problems of such work.

Study Site

Baulárvallavatn (64°54'N, 22°53'W) in western Iceland (Figure 1a) was selected after preliminary examination of a range of lakes in the region to provide a high-resolution palaeoclimate record for the last 1000 years. The site was chosen because it is located only 20 km from the meteorological station at Stykkishólmur which has an observational record dating back to AD 1845, extended to AD 1823 using data from Reykjavík (available at http://www.vedur.is), providing a good opportunity to validate the proxy record over the observational period. Lakes closer to the station were considered to be more affected by human activity and to likely be less sensitive to temperature variations lying

close to sea level. Baulárvallavatn, located at 193 m above sea level, was considered more likely to be temperature sensitive, whilst retaining a reasonable sedimentation rate. Additional site description and data are detailed in Holmes et al. (2009).

Materials and Methods

Fieldwork

A bathymetric profiling of the lake (Figure 1b) was produced by traversing the lake in a boat with a depth sounder and portable GPS. A 70 cm core (BAUL) was obtained from a water depth of 30 m using a UWITEC corer. The core was not taken from the deepest part of the lake (46m) but was from a relatively flat bottomed part of the lake (Figure 1b), as in the deeper areas the lake bottom shelved steeply and potential problems exist with using the Icelandic temperature transfer function on deep (z_{max} > 30m) sites (Axford et al., 2009). The core was returned to the laboratory where it was stored at 4 °C. Other replicate cores were taken from across the basin, and key stratigraphic changes and/or specific measured parameters are reported below.

Sediment geochemistry

On return to the laboratory the core was split in half and analysed using the Itrax micro-XRF core scanner (Croudace et al., 2006) at the British Ocean Sediment Core Research Facility (National Oceanography Centre, Southampton). These analyses provided X-radiographic images and down-core elemental compositional variations at a 200 µm resolution. The XRF data were acquired using a Mo X-ray tube running at 30kV 30mA. A count time of 15 seconds per increment was used.

Chronology

Despite the well documented problems of radiocarbon dating in Icelandic lakes, primarily due to old carbon entering the lake system through terrestrial and/or groundwater pathways, some pilot radiocarbon analyses were attempted on BAUL. Due to a lack of terrestrial macrofossils within the core five bulk sediment subsamples were sent to the Poznan Radiocarbon laboratory for dating, with one level, 47-47.5 cm, also being analysed for the humic acid fraction. A water sample (taken in 2007) was also analysed for its radiocarbon content.

The uppermost samples were freeze dried and analysed for ^{137}Cs by gamma spectroscopy using a well-type coaxial low background intrinsic germanium detector. ^{137}Cs was measured using the 660 keV gamma energy and counting was for 100 ksec for each sample. The efficiency function of the detector was determined using an NPL (Teddington, UK) certified mixed gamma source.

Tephra analyses can be a useful addition to developing chronological models in Iceland (e.g. Boygle 1999; Caseldine et al., 2006), although relatively large volumes of background ash levels can make identifying individual eruptions problematic. In western Iceland relatively few primary ashfalls have been identified (Thordarsson and Höskuldsson, 2008), which is unsurprising given the prevailing westerly winds and that all major volcanic centres, except Snæfellsjökull, are located to the east. Following visual and x-ray inspection of the core, and XRF scanning a number of samples were selected for tephra analyses (cf. Kylander et al., 2012). These samples were sieved (80 and 25 μm) and processed using a heavy-liquid separation method (Turney, 1998) to isolate the 2.3-2.5 g/cm^3 and >2.5 g/cm^3 fractions. Each fraction was prepared onto slides for geochemical analysis by electron microprobe analysis (EPMA). A Cameca SX-100 microprobe housed at the University of Edinburgh was used for this work and the operating conditions followed those outlined in Hayward (2012). In order to derive a chronological model with estimated age uncertainties throughout the core the chronological information (coring date, ^{137}Cs peak and tephra dates) were input into the R package Bchron (Haslett and Parnell, 2008). Bchron (MCMC function, 100000 iterations) fits a compound Poisson-gamma distribution to the increments between the dated levels; these are then used to predict ages for depths through the core. The mean chronology was calculated and is the chronology that is used to plot the downcore data from Baulárvallavatn. The full range of chronological models (10000) provides us with chronological uncertainties for the whole core not usually afforded when using historical tephrochronology.

Magnetic susceptibility

The magnetic susceptibility of discrete samples (0.5 cm freeze dried samples) was measured using a Bartington MS2 Susceptibility system (Dearing, 1994). Both low (χlf) and high (χhf) frequency mass magnetic susceptibility were measured, and percentage frequency dependent susceptibility (χfd%) was calculated.

δ^{13}C, %TOC, and %TN

Bulk sediment organic carbon isotope ratios ($\delta^{13}C_{organic}$), total organic carbon (%TOC) and total nitrogen (%TN) were determined on decarbonated samples using a Carlo Erba Elemental Analyser (NA 1500) attached to a VG Optima mass spectrometer and VG Triple Trap. $\delta^{13}C_{organic}$ values were calculated to the VPDB scale using a within-laboratory standard (BROC) (replication precision of ±0.12‰; 2σ). %TOC and %TN were determined with reference to an Acetanilide standard (replication precision 0.16; 2σ). These values were used to calculate weight C/N ratios.

Diatom and modern water stable isotopes

Samples for $\delta^{18}O_{diatom}$ were prepared using a process of chemical digestion, differential settling, sieving and heavy liquid separation loosely based on Morley et al. (2004). Sediment samples were treated with 30% H_2O_2 at 90°C until reactions ceased (to remove organic material), before using 5% HCl to eliminate any carbonates. Following differential settling, all samples were centrifuged in sodium polytungstate (3Na2WO49WO3.H2O) (SPT) heavy liquid, resulting in the separation and suspension of diatoms from the heavier detrital residue. The purified diatom samples were then sieved at 10 µm and checked for purity using microscopy. Multiple cleans were required to ensure that all tephra shards were removed. Purified diatom samples were analysed for $\delta^{18}O_{diatom}$ using the step-wise fluorination method outlined in Leng and Sloane (2008). The outer hydrous layer of the diatom, known to freely exchange isotopically with water (e.g. Juillet-Leclerc and Labeyrie, 1987), was removed in a pre-fluorination stage using BrF_5 at low temperature. This was followed by a full reaction at high temperature to liberate oxygen that was then converted to CO_2 (Clayton and Mayeda, 1963) and measured for $\delta^{18}O_{diatom}$ using a MAT253 dual-inlet mass spectrometer. All $\delta^{18}O$ values were converted to the VSMOW scale using the within-run laboratory standard BFCmod, and are reported here in per mil (‰). Replication precision for $\delta^{18}O$ is typically +/–0.3‰

Oxygen isotope ($\delta^{18}O$) measurements on water samples were made using the CO_2 equilibration method with an Isoprime 100 mass spectrometer plus Aquaprep device. Deuterium isotope (δD) measurements were made using an online Cr reduction method with a EuroPyrOH-3110 system coupled to a Micromass Isoprime mass spectrometer. Isotope measurements used internal standards calibrated against the international standards VSMOW2 and VSLAP2. Replication precisions are typically +/– 0.05‰ for $\delta^{18}O$ and +/–1.0‰ for δD.

Subfossil chironomids

Samples were prepared for subfossil chironomid analysis using standard techniques (Brooks et al., 2007) including ultrasound treatment (Lang et al., 2003). The head capsules were identified using Hofmann (1971), Wiederholm (1983), Schmid (1993), Rieradevall and Brooks (2001) and Brooks et al. (2007). The chironomid diagram was produced using C2 (Juggins, 2007). Principal components analysis (PCA) was undertaken using Canoco (ter Braak and Smilauer, 2002) and both the Icelandic chironomid-inferred July air temperature transfer function (Langdon et al., 2008) and a combined Norwegian-Icelandic chironomid-inferred July air temperature transfer function (Holmes et al., 2011) were applied to the downcore data using C2 (Juggins, 2007). Bchronproxyplot (Parnell and Haslett,

2008) was used to produce inferred climate reconstructions showing the full range of chronological uncertainty.

Results

Sediment geochemistry

The X-radiographs generated images revealing clear millimetric and sub-millimetric layering (Figure 2). The distinct dark bands correspond to denser mineralogical layers that most likely indicate ash layers or in-wash events. The higher density of such layers may relate to composition and/or finer grain size. The identification of relative density variations of layers at medium to high resolution coupled with the elemental analytical capability permits the potential recognition of marker layers, which were investigated further to try and identify well defined tephra layers (see below). The elemental signatures of the layers seen implied that recognition is easiest with intermediate-acid igneous compositions (co-variation in Si, K, Rb and Zr). Two tephras were identified, both from the X-radiograph and clear peaks in K and Zr, towards the base of the core, at depths of 55-56 cm and 66-67 cm (Figure 2).

Other elemental signatures and ratios can typically be used to help identify variations in clastic input. For example, Si/Ti are typically used to reflect clastic input associated with grain size variations (e.g. Chawchai et al, submitted), although other researchers have argued it can be a proxy for biological silica (BSi) (Johnson et al. 2011; Liu et al. 2013). Si has multiple roles in geochemical processes, being found in siliceous microfossils and mineral material. Given the large amount of mineral materials in Icelandic lake sediments, notably from (often reworked) basalts and related igneous material, the Itrax data was studied to see if we could see evidence for changes in clastic input, which may be driven by changes in precipitation. Zr/Rb ratios were examined, as Rb is commonly associated with clay, while Zr is enriched in coarse silts, hence high Zr/Rb reflect coarse particles (Schillereff et al. 2014). However, the dominant basaltic composition of sediment sources in the Baulárvallavatn catchment makes the use of geochemical proxies for environmental/precipitation changes (e.g. Si/Ti, Zr/Rb) difficult as the Itrax signals for Si and Rb are small (except where there is a contribution from more evolved ash-rich layers of intermediate to silicic composition). So in the current context the Itrax data (geochemistry and radiograph) aid the identification of tephras (especially intermediate-silicic), but elemental profiles do not indicate any clear variations that correlate with other proxies for environmental change.

Chronology

The ^{137}Cs analyses showed a clear peak in levels attributed to 1963 at 2.5 cm depth. Providing a longer chronology for the sediment sequence proved to be problematic. The series of radiocarbon dates showed no regular change through time with all dates providing values between 2600-2100 ^{14}C yr BP (Table 1). A radiocarbon determination of modern lake water (sampled in 2007) showed considerable input of old carbon from the eroding soils in the catchment and there is little reason to believe that such an ageing effect will not have occurred consistently over the last millennium.

Eight samples were selected for tephra analyses. The two visible tephra layers (55-56 cm and 66-67 cm) were geochemically identified as the Landnám (AD871 ± 2; Grönvold et al., 1995) and Sn-1 (1780 ± 35 BP; Larsen et al., 2002) tephras (Figure 3a). Both the basaltic and the rhyolitic component of the Landnám tephra were present. Glass shards from the remaining tephra-rich horizons were geochemically identified as deriving from the Hekla, Snæfellsjökull, Torfajökull, Katla and Veiðivötn volcanic systems (Table 2). The density fractions were dominated by silicic shards (SiO_2 >63%: 2.3-2.5 g/cm^3) and basaltic shards (SiO_2 45-52%: >2.5 g/cm^3). Intermediate shards (53-62% SiO_2) were found in both density fractions. The silicic samples were dominated by shards from Torfajökull (To) and Snæfellsjökull (Sn). These are interpreted as reworked shards from the Landnám and Sn-1 eruptions (and possibly Sn-2 and Sn-3; Jóhannesson et al., 1981) since no younger tephras from these systems are known (Haflidason et al 2000). Silicic shards from Katla (SILK) occur in some samples. These shards are also interpreted as reworked and can either derive from the youngest silicic eruption of Katla, SILK-YN which is dated to 1676 ± 12 BP or the older SILK-N4 (Larsen et al., 2001, Larsen and Eiríksson 2008). These eruptions had lobes extending to the northwest and it is possible that some shards may have reached western Iceland and the catchment of Baulárvallavatn. Intermediate and silicic shards from Hekla occur in most samples, and are especially abundant at 10-11 and 23-24 cm. However, given the abundance of reworked shards from other older silicic eruptions, a significant part of the Hekla shards can be expected to be reworked, in particular the highly silicic shards (SiO_2 >65%). Basaltic tephra from all the main basaltic volcanic systems occur in the samples, i.e. Grímsvötn, Veidivötn and Katla. However, the dominant basaltic component has high Al_2O_3 (c. 15-16 wt %) and K_2O (c. 0.8-1.2 wt %) content and has affinities to basaltic lavas from the Snæfellsnes Volcanic Zone, mostly those of the Ljosufjoll system (Kokfelt et al, 2009; Steinthorsson et al. 1985 and unpublished data). It could, however, also originate from the older hyaloclastite formations in the vicinity of the lake and be blown or washed in to the lake.

All analyses are listed in Table 2 and details can be found in the Supplementary Material. The tephra-based age model assumes that some of the analysed tephra shards are primary and represent true isochrons in the sediment. We are aware, however, that the majority of the shards are likely reworked by catchment processes. For example, several of the shards with Hekla affinity could be reworked from prehistoric eruptions which had a westward distribution, e.g. Hekla-B and Hekla-C (Larsen and Eíriksson, 2008). Although each sample contained a mixture of shards thought to originate from different volcanic centres, we pinpoint the specific volcanic eruption based on the abundance of shards and the known dispersal patterns of historical eruptions in Iceland. For example, two samples (3-4 cm and 14-15 cm) contain relatively large amounts of shards from Veiðivötn, but despite these relatively high numbers, we are not aware of any historical eruptions from this centre being dispersed towards northwest Iceland, and hence interpret them as reworked shards from the basaltic part of the Landnám tephra. The samples at 3-4 cm contain a numbers of basaltic grains from Katla. Tephra was dispersed widely from the eruption of Katla in 1918 including one lobe reaching Snæfellsnes (Larsen et al., 2014) and we suggest that the shards in the 3-4 cm sample derive from that eruption. The sample at 10-11 cm has abundant tephra from several volcanic systems. Silicic shards from Hekla, however, are one of the most abundant components within this sample and it is possible that some of these shards (SiO_2<65%) derive from the relatively large eruption in 1766. Tephra-fall was reported from north and northwest Iceland but the Hekla 1766 deposit has as yet, not been found on Snæfellsnes (cf. Larsen et al., 2014). Tephra from the eruption of Katla in 1721 reached western Iceland (Larsen et al., 2014) and we suggest that the few Katla shards in the 14-15 cm may relate to this event. The same sample also contains a reasonable number of shards from the Hekla volcanic system which may be derived from Hekla-1693 event. The Hekla-1693 tephra was carried towards the northwest and has recently been confirmed in lake sites in the Western fjords (Langdon et al., 2011). The sample at 23-24 cm is more difficult to assign to a certain eruption. More than half of the analyses suggest an origin in the Hekla system and indeed several of the analyses show similarities with the Hekla 1510/Loch Portain B tephra, found in Scotland and Ireland (Figure 3b; Dugmore et al., 1995; Pilcher et al., 1996). Reports from Iceland, however, are scarce (Larsen et al., 2014) and indicate a main dispersal axis towards the southwest. Nonetheless, given the good matches identified in Figure 3b, we use Hekla 1510 in our age model (Table 2). Only a few analyses are available from 29-30 cm and the shards with Hekla affinity do not allow a secure correlation with any of the historic eruptions of Hekla. It is possible, however, that the Hekla 1341 eruption reached the area since a tephra fall was reported in west and northwest Iceland at this time (Thorarinsson 1967). We are unable to pinpoint a volcanic eruption for sample 33-34 cm.

The tephra dates (Table 2) were used alongside the ^{137}Cs data and coring date to produce a chronological model using Bchron, which is presented in Figure 4. Given the uncertainties associated with which Hekla eruption might be represented by the samples at 23-24 cm and 29-30 cm (as noted above), three age models were developed, taking into account the maximum uncertainties (i.e. oldest and youngest possible tephras for the less certain Hekla levels). The most parsimonious model is shown in Figure 4, with Hekla 1510 assigned to 23-24 cm, and Hekla 1341 assigned to 29-30 cm. This approach allows the estimation of chronological uncertainty through the core; chronological uncertainty is smaller closer to the tephra layers where the chronology is constrained by the most confident tephra matches. There is a reasonably constant sedimentation rate of approximately 0.05 cm yr^{-1} during the past 1000 years. Although beyond the main timescale focus of this study it can be seen that prior to Settlement the sedimentation rate was lower (c. 0.02 cm yr^{-1}), as would be expected from other Icelandic lake sites.

%TOC, C/N, organic carbon isotope composition and magnetic susceptibility data

The %TOC, C/N, $\delta^{13}C$ and magnetic susceptibility data (Figure 5) show clear changes through the record. Isolated spikes (low %TOC values at AD 870 and AD 1341) reflect the dominant input of isolated tephra horizons from single eruptions; details also identified from the Itrax elemental data (cf. Kylander et al., 2012). Apart from the effect of the Sn-1 tephra (c. AD 170) prior to Settlement the sedimentary records are relatively uniform implying little variability in catchment dynamics through time, with a $\delta^{13}C$ value around –26‰, %TOC of around 3% and C/N of c. 9. After Settlement all these proxies show significant variations with a trend to increasing %TOC, lower $\delta^{13}C$, reaching <–27‰ at the surface, and C/N values of between 10 and 12, though these decrease to around 9.5 at the surface. Changes are less apparent in the magnetic susceptibility record with greater variability before the last millennium, but slightly higher low frequency susceptibility values following Settlement. A short lived peak in frequency dependent susceptibility c. AD 1210 stands out, which also corresponds with an increased peak in %TOC, C/N and increase in $\delta^{13}C$.

Modern water and diatom stable isotope composition

Waters for isotope analysis were sampled soon after ice out (April/May 2007), which likely reflects winter precipitation, and also from the preceding summer, July 2006, to compare any seasonal differences. The winter waters had lower $\delta^{18}O$ compared to summer, and Baulárvallavatn and the other nearby lakes all plot along the global meteoric water line (GMWL) (Figure 6), indicating the lake waters represent seasonal variation in precipitation and a sub-annual lake water residence time (St Amour et al., 2010). Two of the lakes, Svínavatn and Saurarvatn, have summer isotope

compositions that define a local evaporation line (LEL). Both these lakes are smaller and shallower than Baulárvallavatn, suggesting that these lakes evaporate in the summer but are recharged in the winter.

The diatom $\delta^{18}O$ data (Figure 5f) cover the period AD 100-1300. No samples were analysed post-AD1300 as the background tephra concentrations were too great, prohibiting clean preparations from being obtained, despite several attempts. The data pre-AD 1200 vary between +28.4 to +32‰, with a mean value of +29.7‰. A peak value of +32‰ is centred on AD 295, with low values (around +29‰) centred pre-AD 200, and around AD 540, AD 930, and AD 1140. Post-AD 1200, there is a short-lived increase to +40‰ around AD 1205 before a decrease to +26‰, the lowest value measured in the core, c. AD 1295. The extreme high value of +40‰ was replicated in multiple sample analyses and compared with spikes in other sedimentological proxies (Figure 5). The isotopic composition of present day waters ($\delta^{18}O$, δD) was measured from Baulárvallavatn and nearby lakes (Figure 6).

Chironomid stratigraphy

Forty six chironomid taxa were identified in the Baulárvallavatn core; the percentage diagram (Figure 7) shows selected taxa only. The chironomid assemblage is dominated by *Heterotrissocladius grimshawi*-type (between 24-73%) with *Psectrocladius sordidellus*-type (2-32%), *Chironomus anthracinus*-type (0-32%), *Paracladopelma* (0-18%), *Eukiefferiella* (0-17%) and *Micropsectra* (0-14%) the next most abundant taxa. These taxa commonly occur in high levels in many other Icelandic lakes (Langdon et al., 2008). The majority of the chironomid taxa present occur throughout the core and although there are no major changes in terms of one taxon replacing another, there are some clear trends and oscillations in certain taxa throughout the core. The base of the sequence is dominated by relatively high abundances (although variable) of thermophilous taxa such as *C. anthracinus*-type and *P. sordidellus*-type that lasts until the early 1300s. There is a noticeable change in chironomid assemblage c. AD 1450-1520, with an increase in *Chaetocladius*. The period from late AD 1500 to mid AD 1800 has a relative increase in *Diamesa*, which typically represent cooler conditions. Head capsule concentration ranged between 19 and 187 head capsules g^{-1}, with the peak concentration of 187 head capsules g^{-1} occurring at c. AD 1220.

Chironomid-inferred temperature reconstructions

The most commonly used method to produce a temperature reconstruction from downcore data is to apply a transfer function developed using a modern surface sample training set (e.g., Caseldine et

al., 2006; Axford et al., 2007; Langdon et al., 2008; Gathorne-Hardy et al., 2009). The mean July air temperature reconstruction produced by applying the Icelandic transfer function (Langdon et al., 2008) to the Baulárvallavatn data (Figure 7) shows a range of reconstructed temperatures of 2.5 °C (maximum = 9.7 °C; minimum= 7.2 °C) during the past 1000 years. The chironomid samples covering the period 1961-1990 infer a mean July air temperature of 8.59 °C. When this is compared with the modelled mean July air temperature of 9.62 °C from 1961-1990 (Björnsson et al. 2003) it is clear there is an under-prediction of over 1 °C (just within the model RMSEP of 1.1 °C). A combined Norwegian-Icelandic transfer function (Holmes et al., 2011) was also applied to the data (Figure 7), as this model may produce more realistic temperature reconstruction (Holmes et al., 2011). The results from this approach were similar to those produced using the Icelandic transfer function, though the range of reconstructed temperatures was slightly smaller (2.2 °C). When compared to the Stykkishólmur instrumental temperature data (corrected for altitude) both the chironomid-inferred temperature reconstructions produce values which under-predict by between 0.5 °C and 1 °C. It should be remembered that the chronological uncertainty precludes validation of the chironomid data against the instrumental data, and therefore only a visual comparison is used here. It is clear from this approach that the trends and pattern of the C-IT reconstructions are not similar to the instrumental data. Over the whole period studied both the chironomid-inferred temperature reconstructions suggest that the second half of the millennium had higher temperatures, with the warmest period occurring between c. AD 1600-1840 and the warmest temperature reached c. AD 1800. This is contrary to what is known about the climate of this time from other data sources; as a result the chironomid-inferred temperature reconstructions are not interpreted any further (cf. Axford et al., 2009) and possible reasons for this are discussed below.

Ordination of the chironomid data

Detrended correspondence analysis (DCA) revealed a gradient of 0.98 standard deviation units resulting in the linear treatment of the data in further analyses. PCA was carried out and PCA axis 1 scores are shown in Figures 7 and 8. The PCA axis 1 scores show a remarkable similarity to other palaeoclimatic proxy data covering the same time period (Figure 9) and have been interpreted as providing a palaeoclimatic reconstruction with higher PCA axis 1 scores reflecting warmer temperatures and lower PCA axis 1 scores reflecting cooler temperatures (see below for discussion).

Figure 8 was produced using Bchronproxyplot in Bchron (Haslett and Parnell, 2008) and shows the PCA axis 1 scores plotted using a sample of 1000 chronologies (grey lines) produced for the core. The PCA axis 1 scores are also plotted against the mean chronology (black line); using this, the

highest PCA axis 1 score occurred c. AD 1060 while the lowest score occurred c. AD 1780. It can be seen, when taking into consideration chronological uncertainty, that the period c. AD 1000 to c. AD 1550 has higher PCA axis 1 scores (and therefore was warmer) than the period c. AD 1550 to AD 2006. Looking at the grey plots it seems that the latter period has more variability, though this is possibly due to tighter chronological constraint during this time. It is also clear from this diagram that using data such as these (e.g. non-varved, non-annually resolved data) to perform calibration against instrumental data would be unwise, therefore this has not been attempted as part of this study. A better chronologically constrained core would be needed in order to do this.

Discussion

The sediment record and lake history

By combining the %TOC, C/N, $\delta^{13}C$ and sedimentation rate results it is possible to infer the changing nature of sedimentation into the lake over the last millennium. Prior to Settlement (~AD 874) sedimentation was low at 0.02 cm yr^{-1} and %TOC reflects lake productivity as seen in C/N values below 10 (algal material), and $\delta^{13}C$ around –26‰ (typical of aquatic plants, Figure 5). Following Settlement the rate of sedimentation increased by a factor of 2.5 to 0.05 cm yr^{-1}, with a rapid doubling in %TOC and a change in C/N to over 10 (suggesting a terrestrial component). From around AD 1400 there was a further gradual rise in C/N peaking at the end of the 19th century, mirroring a change in $\delta^{13}C$ to –27‰ (values typical of terrestrial plants). The %TOC, C/N and $\delta^{13}C$ records correlate well (Figure 9). As %TOC increases, so does C/N, indicating that the increase in %TOC is driven by in-wash of terrestrial organic matter (higher C/N than algae) and hence old soil carbon and terrestrial plant fragments were likely continuously added to the lake system (cf. Axford et al., 2009; Gathorne-Hardy et al., 2009; Geirsdóttir et al., 2009b). The lower $\delta^{13}C$ with increased %TOC corroborates this interpretation (Langdon et al. 2010). The alternative explanation, of increasing algal productivity, would have led to increases in $\delta^{13}C$ (not decreases), as algae preferentially utilise ^{12}C (Meyers and Teranes, 2001). Interestingly, it is this latter relationship that Geirsdóttir et al. (2009b) found at Haukadalsvatn, with an associated increase in BSi, suggesting that the lake had undergone a phase of enhanced productivity, perhaps stimulated through the input of increased organic matter.

The ability of quite large plant remains to be deposited across the lake can be observed during spring melt when rivers in flood and small debris flows extend over the remaining ice cover. It seems likely that isolated peaks in $\delta^{13}C$ could indicate extreme winter/spring flood or flow events that move material directly onto ice over the deeper parts of the lake, as a suite of cores from across the lake

showed occasional lenses of poorly humified plant debris. The importance of redeposited C in the lake, both as particulate and dissolved material is evident from the radiocarbon analyses. The lake water currently has a radiocarbon age of almost 3500 years and this, coupled with redeposited plant and/or soil remains from the catchment, gives the relatively uniform set of ages for the lake sediment. Sufficient macrofossil remains for dating were not available from the selected core, although in an adjacent core a date of 2120±30 ^{14}C BP was obtained from moss remains near the base of the core, a date that fits well with the depth and age of the tephra Sn-1 in the sampled core. Nonetheless, given the evidence of increased erosion from the catchment there is no guarantee that ages from terrestrial macrofossils will be contemporaneous between the date of inwash and the material being transported.

The increased soil erosion through the last millennium at Baulárvallavatn (increase in %TOC etc.) is most likely due to one, or both, of two processes. Settlements at lower altitudes typically introduced sufficient grazing around the lake to initiate severe and persistent soil erosion (e.g. Simpson et al., 2004; Lawson et al., 2007), and this is likely a background effect. Superimposed on this are changes in climate, as cooler dry summers can reduce vegetation cover, enhancing aeolian erosion and transport of organic matter into the lake (Geirsdóttir et al., 2009b). Increases in %TOC can thus be interpreted as moving towards cooler summers, with dry windy winters, as exemplified by Geirsdóttir et al. (2009b). Following this line of argument, it seems likely that significant shifts in the δ^{13}C record, as at c. AD 1240 and AD 1550, may well represent a climate driven signal, with the highest %TOC and C/N and the lowest δ^{13}C (outside the most recent sediments) being found around AD 1750, a period interpreted as particularly cold (see later discussion) (Figure 9). The emerging interpretation is thus of a lake subject to enhanced organic input derived from the surrounding catchment over the last millennium, in contrast to preceding centuries, which most likely reflects in part an anthropogenic signal, but crucially, a strong climate signal through increased erosion of a less resilient surface soil.

Climate variability of the last 1000 years

The $\delta^{18}O_{diatom}$ record (Figures 5 and 9) is interpreted in terms of changes in seasonal precipitation following the arguments outlined in Rosqvist et al. (2013), as Baulárvallavatn is a hydrologically open lake (low residence time, non-evaporative). When cool Arctic air masses dominate, lake waters have low δ^{18}O, whereas higher δ^{18}O would result from southwesterly derived north Atlantic air masses (GNIP database, 2014). Rosqvist et al. (2013) argue that for their $\delta^{18}O_{diatom}$ records from Sweden, temperature impacts on the stable isotope record are likely negligible, as the summer temperature

changes over the last 1000 years are in the order of 1 °C (Esper et al., 2012). Given the net effect of an increased condensation temperature is in the order of +0.5‰/°C (following Rosqvist et al., 2013), and the amplitude of the $\delta^{18}O_{diatom}$ record is 3.6‰ (pre AD 1200), it is likely that temperature is not the main driver of this isotopic signal, compared to changing source of precipitation. The relatively high values around AD 300, AD 650 and from AD 950-1100 likely suggest summer precipitation (south westerly sources) dominated compared to winter Arctic precipitation. Conversely, around AD 540, AD 930 and AD 1150, winter precipitation was likely relatively dominant. The sharp peak just after AD 1200, with extremely enriched stable isotopes, can be explained as a period of high evaporation, or higher summer rainfall (with higher $\delta^{18}O_{diatom}$) and lower winter rainfall (lower $\delta^{18}O_{diatom}$). In the former scenario of higher evaporation the lake level may have dropped sufficiently to cause the lake to become effectively closed, thus increasing $\delta^{18}O_{diatom}$ further by higher evaporation (Leng and Marshall, 2004). The final sample in the $\delta^{18}O_{diatom}$ dataset, around AD 1300 has the lowest $\delta^{18}O_{diatom}$, and thus is indicative of a shift to relative dominance of winter precipitation compared with summer.

The $\delta^{18}O_{diatom}$ data and interpretation of the sedimentological proxies fits well with the chironomid response (Figure 9). However, it is clear that the transfer function results do not correspond well with the sedimentological data, given they show increased warming between c. AD 1600-1850, when the other proxies suggest enhanced cooling. This is likely related to the increased %TOC, which typically is associated with increased productivity and warming temperatures (e.g. Velle et al., 2010). However, this relationship between productivity and climate can decouple, as argued in Brooks et al. (2012). It is decoupled in the Icelandic transfer function (Langdon et al., 2008), as %TOC plots orthogonal to summer temperature. The Langdon et al. (2008) model includes many lowland lakes, where relatively high levels of organic productivity are associated with warmer temperature lakes. Nonetheless, the large increases in %TOC in Baulárvallavatn, which are likely associated with cooler summers (*cf*. Geirsdóttir et al., 2009b), does seem to affect the transfer function performance in relation to the presence of a strong secondary gradient (Juggins, 2013), and it is thus not surprising that sensible quantitative results are not generated. There are a number of semi-terrestrial taxa (e.g., *Chaetocladius*, *Limnophyes*, *Paraphaenocladius*/*Parametriocnemus* and *Pseudosmittia*) present at various points in the Baulárvallavatn chironomid record which could support the suggestion of increased catchment erosion due to cooler summers and drier winter conditions. These taxa are present in low numbers in the Icelandic training set and have relatively warm temperature optima (Langdon et al., 2008) and may be a factor contributing to the unreliable temperature reconstruction produced using the Icelandic transfer function, while an ecological interpretation (supported by the

PCA analyses) supports the assertion that they are responding to temperature. Despite the problems with transfer functions outlined by Juggins (2013), there is strong evidence that chironomids are sensitive to summer temperatures in Iceland (Caseldine et al., 2003, 2006; Langdon et al., 2008, 2011; Holmes et al., 2011) and hence in *some* lakes provide a valid temperature reconstruction. Axford et al. (2009) argued for a link with August temperatures through a calibration with the Stykkishólmur temperature record based on a relatively small sample of 10 data points. These analyses showed a stronger relationship with mean annual temperature (possibly acting via the effect of ice thickness and melt-out date on chironomid growing season length and emergence date), but August temperatures were reconstructed due to the known relationship between summer air and water temperature and chironomids (Axford et al., 2009). It has not been possible to carry out a similar calibration exercise here, due to chronological uncertainty in the upper sediments, but the variability seen in this record, compared to other independent proxy data from both terrestrial and marine sources (Figure 10), is strongly suggestive of a climate signal, as for instance is also shown in the high altitude site at Mýfluguvatn (Langdon et al., 2011), where there is co-variation between the C-IT and DCA reconstructions. Thus, although not providing a calibrated quantitative record for Baulárvallavatn the PCA record does provide additional faunally-based climate evidence for the last millennium and has a much stronger chronological control in terms of known uncertainties, than at any other Icelandic site that covers the last 1000 years. Clear periods of long-term trends can be identified within the last 1000 years within the chironomid and other records (Figure 10; inferring climate (summer temperature) from the chironomid PCA analyses), and group broadly into four main phases:

AD 1020-1310

By comparison with the mid- to late 20th century it seems likely that temperatures were slightly warmer in general during this period. The highest temperatures were seen as an isolated peak around AD 1060 with cooling to a clear trough between AD 1130 and AD 1180. The first half of the 13th century was warm, comparable to the end of the 20th century, before a second dip after AD 1260 reaching a minimum around AD 1300. In summary the mean values between AD 1020 and AD 1310 could be interpreted as warmer than the *overall* 20th century mean with two, possibly three phases of decadal cooling centred on c. AD 1060-70, AD 1140-80 and AD 1270-1310.

AD 1310-1560

Values are relatively stable between AD 1310 and AD 1510, cooler than in the preceding period, but still notably warmer that the second half of the millennium. The period ends though with a sharp

decline to the second lowest values in the record centred on AD 1535 before returning to values seen in the rest of the period at c. AD 1555.

AD 1560-1810

From AD 1560 the PCA record suggests a consistent decline in temperatures to a minimum around AD 1780 with the lowest temperatures in the record. There is no evidence of any even short-term return to those temperatures preceding AD 1560, with the coldest phase being marked between AD 1680-1810.

AD 1810 – late 20th century

Apart from an early single peak around AD 1815 values are generally lower than before AD 1560, although warmer than in the preceding two centuries. The trend from c. AD 1900 onwards is for rising temperatures with variability between samples comparable to those throughout the record. By the most recent sample, representing the end of the 20th century and the beginning of the 21st century, values rise to those found almost a thousand years previously.

When the full range of chronological uncertainty is considered the four phases of climatic conditions are still valid (Figure 8), and it is clear that the first half of the millennium experienced warmer climatic conditions than the second half, though with a return to the warmer climate occurring in the last c. 100 years. Comparison of existing records with other terrestrial data and especially offshore data reveal broad scale agreements (Figure 10). Axford et al. (2011) showed significant correlations across marine records around Iceland, and that sites in the west of Iceland (and offshore) relate strongly to the Irminger Current and North Atlantic Drift over time (Ólafsdóttir et al., 2010). Regional climatic variations across Iceland during the Holocene have been apparent from a number of studies, especially for earlier in the Holocene (Caseldine et al., 2006; Axford et al., 2007), and Axford et al. (2011) argue that sites in the north of Iceland may be relatively less coupled to the west, although the nature of the seasonal drivers enhancing this variability over millennial timescales is not clear. The Baulárvallavatn record reinforces some of the broader climate reconstructions for the last millennium: peak warmth in the 11th century AD, persisting with decadal variability to the mid-13th century, a period of cooling in the early 14th century with quite variable but not cold temperatures until a sharp drop c. AD 1535 preceding a more steady decline in temperatures through the 17th and 18th centuries, leading to a minimum around AD 1780-1800. Temperatures begin to recover through the 19th and into the 20th century eventually producing conditions comparable to those at the beginning of the millennium (cf. Miller et al., 2012).

The decadal resolution of the chironomid data appears to clearly capture a low frequency signal with multi-decadal variability superimposed on it and occasional rapid excursions. This low frequency signal compares well with the Haukadalsvatn low frequency signal and as such appears to reflect the orbitally driven decrease in summer insolation for this region (PAGES 2k Consortium, 2013). A clear change is observed around the start of the 13th century, shown by the initiation of a new directional trend in the chironomid PCA reconstruction, which correlates with a change in magnetic susceptibility and sedimentary proxies around AD 1210. The reconstructed cooling c. AD 1270-1310 coincides with a period of decreased summer temperature and increased ice growth (AD 1275-1300) in Arctic Canada (Miller et al., 2012), and the beginning of a period of increased varve thickness in Hvítárvatn (Larsen et al. 2011), thought to be the result of climatic changes started by a period of explosive volcanism and propagated by sea-ice and ocean feedbacks (Miller et al., 2012). Andrews et al. (2009) observe a major change in marine climate variability at this time, and it could be interpreted as marking the climate system reorganisation and initial decline into climates associated with the Little Ice Age.

The variability of the chironomid PCA axis 1 scores can be investigated further. Some periods exist of relatively stable conditions with variation around a mean value, while at other times there are relatively rapid shifts in regime between these stable periods, and short term severe 'events' likely to be of sub-decadal duration. In order to examine this further, the PCA reconstruction was smoothed using a negative exponential smoother; the analyses used a polynomial regression and weights were computed from the Gaussian density function (sampling proportion 0.1, polynomial degree 1). To best understand the nature of the variability in the chironomid data, the residuals of the smoothed PCA were analysed through rolling windows of 50 years, 100 years and 200 years. The results of each rolling window test were similar, and the 100 year dataset have been plotted against North Atlantic Oscillation (NAO) variability (Trouet et al. 2009) for the last 1000 years (Figure 11). The chironomid record shows a centennial scale variability that is persistent throughout the whole of the last millennium. This variability is based on the residuals, and so exists on top of the long-term trends noted above. Comparison with the NAO reconstruction from Trouet et al. (2009) shows a clear match between the records (within the errors of the age model), especially between AD 1400-2000. Before this, the oscillations in the chironomids pervade, while the NAO index shows a period of relatively less variability but was in a phase of enhanced dominant mode. Interestingly the magnitude of the variability of the chironomids is relatively large, and increasing from AD 1000-1650, but thereafter reduced in magnitude. The phase of positive NAO is linked to enhanced zonal

633 flow, with westerlies delivering warmer weather to continental Europe, with the storm track moving
634 further north and so Iceland is warmer but wetter in winter. In more negative phases of the NAO sea
635 ice builds up around Iceland so it is cooler but drier. A wetter winter will likely increase snowfall
636 around Baulárvallavatn, which would be melted off in warmer summers, influencing chironomid
637 populations which typically respond to summer temperatures. Thus, the controls of NAO on
638 Icelandic temperature seem to match the variability of the chironomid faunas on a multi-decadal to
639 centennial scale. Other links have been made between NAO and aquatic ecosystems (e.g. Straile,
640 2002; Blenckner et al. 2007), with the dominant argument being for a link through food-webs
641 primarily controlled by faster population growth of algae in warmer waters. The peaks and troughs
642 in NAO at the multi-decadal scale (i.e. warmer/cooler climate) clearly relate to enhanced variability
643 of chironomid communities, suggesting that as the food-web is altered through NAO driven
644 mechanisms, the chironomids also respond in terms of relatively high levels of internal trophic level
645 variability.
646
647 *Wider significance and broader issues*
648 Examination of the Baulárvallavatn record, especially in comparison with the other available
649 Icelandic terrestrial data (Figure 10), raises a number of issues concerning how best to derive the
650 desired quantitative high resolution terrestrial temperature record that is really needed to compare
651 with onshore and offshore records elsewhere. It seems likely that at present chironomid-based
652 temperature reconstructions provide the best opportunity for calibrated quantitative data but it is
653 not clear whether a transfer function or calibrated PCA/DCA approach offers the best route (e.g.,
654 Velle et al., 2010; Brooks et al., 2012; Juggins, 2013; Berntsson et al., 2014). For some lakes the C-IT
655 training set based methodology, however the training set is derived (Holmes et al., 2011), does not
656 appear to be able to reflect likely real temperature changes. Looking for variability in the
657 palaeorecord using PCA/DCA seems to be more appropriate, though it is reliant on accurate and
658 precise chronologies. Alternatively, in some lakes the secondary gradients may be too strong to rely
659 overly on transfer function derived C-IT (Berntsson et al., 2014). If it is assumed that such faunal
660 approaches are the optimal choice then the pressing need is to establish the types of lakes that are
661 best suited. It may be that smaller, higher lakes are more sensitive to temperature change (e.g.
662 Langdon et al. 2011), as they are relatively buffered against human impact. Low altitude, large and
663 deep lakes such as Haukadalsvatn (Geirsdóttir et al., 2009b) and Lögurinn (Striberger et al., 2012)
664 offer important opportunities for proxies such as BSi and %TOC but calibration to temperature may
665 prove difficult, as human activities are likely to impact these proxies, although in the latter case the
666 presence of a chironomid fauna may eventually prove to provide a suitable temperature record.

Smaller lakes at relatively low altitudes have been shown to provide sensitive C-IT reconstructions, despite the possible influence of settlement (e.g. Holmes, 2008; Gathorne-Hardy et al. 2009). It remains to be seen whether high productivity (hence relatively high sample resolution), air temperature sensitive lakes can be found at high enough altitudes to meet the necessary criteria. As such the approach followed at Baulárvallavatn offers a promising opportunity for further development at sites with comparable or better dating control, and for which a well developed quantitative recent record would provide the sort of robust calibration required to produce a high quality temperature reconstruction. The challenge remains to produce the sort of high resolution calibrated data set for temperature that both offshore records and modelling studies merit but it is only by the detailed analysis of sites considered potentially suitable that the most valuable records will be discovered.

Acknowledgements

We would like to thank Gareth Thompson for help in the field and with preparing the diatom stable isotope samples and running the sedimentological analyses. Hilary Sloane, Carol Arrowsmith and Chris Kendrick are thanked for running the stable isotope analysis. We thank Tomasz Goslar for discussion with the interpretation of radiocarbon dates. Andrew Parnell is thanked for his help with the R package Bchron, particulary Bchronproxyplot. Helen Ward and Gareth James are thanked for preparing the tephra samples for microprobe analysis. Chris Hayward at the Tephra Analytical Unit, University of Edinburgh is thanked for help with tephra analyses. We are very grateful to Sigurður Steinþórsson for his unpublished analyses on the Ljósufjöll system from the geochemical data base at Science Institute, analyst Niels Oskarsson. The Southampton Cartographic unit is thanked for preparing the figures.

Funding

The work described in this manuscript was undertaken through the MILLENNIUM project, which focused on better understanding the European climate of the last Millennium. The project was funded by the EU through FP6. We thank the funders, but also the project PI, Danny McCarroll, as well as the WP3 leader Sheila Hicks, plus all colleagues who worked under the Millennium project for stimulating and fruitful scientific discussion.

699 **References**

700 Andrews JT, Darby D, Eberle D et al. (2009) A robust, multisite Holocene history of drift ice off
701 northern Iceland: implications for North Atlantic climate. *The Holocene* 19: 71-77.
702 Axford Y, Miller GH, Geirsdóttir, Á et al. (2007) Holocene temperature history of northern Iceland
703 inferred from subfossil midges. *Quaternary Science Reviews* 26: 3344-3358.
704 Axford Y, Geirsdóttir Á, Miller GH et al. (2009) Climate of the Little Ice Age and the past 2000 years in
705 northeast Iceland inferred from chironomids and other lake sediment proxies. *Journal of*
706 *Paleolimnology* 41: 7-24.
707 Axford Y, Andresen CS, Andrews JT et al. (2011) Do paleoclimate proxies agree? A test comparing 19
708 late Holocene climate and sea-ice reconstructions from Icelandic marine and lake sediments.
709 *Journal of Quaternary Science* 26: 645-656.
710 Berntsson A, Rosqvist GC and Velle G (2014) Late-Holocene temperature and precipitation changes
711 in Vindelfjällen, mid-western Swedish Lapland, inferred from chironomid and geochemical data. *The*
712 *Holocene* 24: 78-92.
713 Björnsson H (2003) *The annual cycle of temperature in Iceland: the 1961–1990 average*. Technical
714 Report, Icelandic Meteorology Office.
715 Boygle JE (1999) Variability of tephra in lake sediments, Svinavatn, Iceland. *Global and Planetary*
716 *Change* 435: 129-149.
717 Blenckner T, Adrian R, Livingstone DM et al. (2007) Large-scale climatic signatures in lakes across
718 Europe: a meta-analysis. *Global Change Biology* 13: 1314-1326.
719 Brooks SJ, Langdon PG and Heiri O (2007) *The Identification and Use of Palaearctic Chironomidae*
720 *Larvae in Palaeoecology*. QRA Technical Guide No. 10. Quaternary Research Association, London.
721 Brooks SJ, Axford Y, Heiri O et al. (2012) Chironomids can be reliable proxies for Holocene
722 temperatures: A comment on Velle et al. (2010). *The Holocene* 22: 1495-1500.
723 Caseldine CJ, Geirsdóttir Á and Langdon PG (2003) Efstadalsvatn – a multi-proxy study of a Holocene
724 lacustrine sequence from NW Iceland. *Journal of Paleolimnology* 30: 55-73.
725 Caseldine CJ, Langdon PG and Holmes N (2006) Early Holocene climate variability and the timing and
726 extent of the Holocene thermal maximum (HTM) in northern Iceland. *Quaternary Science Reviews*
727 25: 2314-2331.
728 Chawchai S, Kylander M, Chabangborn A, et al. (submitted) An example of commonly used XRF core
729 scanning based proxies for organic rich lake sediments and peat. *The Holocene*
730 Clayton RN and Mayeda TK (1963) The use of bromine pentafluoride in the extraction of oxygen
731 from oxides and silicates for isotopic analysis. *Geochimica et Cosmochimica Acta* 27: 43-52.

Croudace I, Rindby A and Rothwell R (2006) ITRAX: description and evaluation of a new multi function X-ray core scanner. In: Rothwell RG (ed) *New techniques in sediment core analysis: Geological Society London Special Publication* 267, pp. 51–63.

Cunningham L, Austin WEN, Knudsen KL et al. (2013) Reconstructions of surface ocean conditions from the northeast Atlantic and Nordic seas during the last millennium. *The Holocene* 23: 921-935.

Dearing JA (1994) *Environmental Magnetic Susceptibility*. Chi Publishing, Kenilworth.

Dugmore AJ, Larsen G, Newton AJ (1995) Seven tephra isochrones in Scotland. *The Holocene* 5: 257–266.

Esper J, Büntgen U, Timonen M et al. (2012) Variability and Extremes of Northern Scandinavian summer temperatures over the Past Two Millennia. *Global and Planetary Change* 88-89: 1-9.

Gathorne-Hardy FJ, Erlendsson E, Langdon PG et al. (2009) Lake sediment evidence for late-Holocene climate change and landscape erosion in western Iceland. *Journal of Paleolimnology* 42: 413–426.

Geirsdóttir Á, Miller GH, Axford A et al. (2009a) Holocene and latest Pleistocene climate and glacier fluctuations in Iceland. *Quaternary Science Reviews* 28: 2107-2118.

Geirsdóttir Á, Miller GH, Thordarson T et al. (2009b) A 2000 year record of climate variations reconstructed from Haukadalsvatn, West Iceland. *Journal of Paleolimnology* 41: 95 115.

Grönvold K, Óskarsson K, Johnsen SJ et al. (1995) Tephra layers from Iceland in the Greenland GRIP ice core correlated with oceanic and land sediments. *Earth and Planetary Science Letters* 135: 149–155.

Gudmundsdóttir, ER, Larsen, G, Eiríksson, J (2012) Tephra stratigraphy of the North Icelandic shelf: extending tephrochronology into marine sediment off North Iceland. *Boreas* 41, 719-734.

Haslett J and Parnell AC (2008) A simple monotone process with application to radiocarbon-dated depth chronologies. *Journal of the Royal Statistical Society: Series C (Applied Statistics)* 57: 399-418.

Hayward CL (2012) High Spatial Resolution Electron Probe Microanalysis of Tephras and Melt Inclusions without beam-induced chemical modification. *The Holocene* 22: 119-125.

Hofmann W (1971) Zur Taxonomie und Palökologie subfossiler Chironomiden (Dipt.) in Seesedimenten. Ergebnisse der Limnologie, Archiv für Hydrobiologie Beiheft (International Vereinigung für theoretische und angewandte Limnologie, Stuttgart) 6: 1–50.

Holmes N (2008) Validation of chironomid-inferred temperature reconstructions in Iceland: the potential for reconstructing quantitative changes in Holocene climate. *Geographica Helvetica* 63: 4-14.

Holmes N, Langdon PG and Caseldine CJ (2009) Subfossil chironomid variability in surface sediment samples from Icelandic lakes: implications for the development and use of training sets. *Journal of Paleolimnology* 42: 281-295.

766 Holmes N, Langdon PG, Caseldine CJ et al. (2011) Merging chironomid training sets: implications for
767 palaeoclimate reconstruction. *Quaternary Science Reviews* 30*:* 2793-2804.
768 Jóhannesson H, Flores R and Jónsson J (1981) A short account on the Holocene tephrochronology of
769 the Snæfellsjökull volcano, Western Iceland. *Jökull* 31: 23-30.
770 Johnson TC, Brown ET and Shi J (2011) Biogenic silica deposition in Lake Malawi, East Africa over the
771 past 150,000 years. *Palaeogeography, Palaeoclimatology, Palaeoecology* 303: 103-109.
772 Juggins S (2007) *C2 User guide. Software for ecological and palaeoecological data analysis and*
773 *visualisation*. University of Newcastle, UK.
774 Juggins S (2013) Quantitative reconstructions in palaeolimnology: new paradigm or sick science?
775 *Quaternary Science Reviews* 64: 20-32.
776 Juillet-Leclerc A. and Labeyrie L (1987) Temperature dependence of the oxygen isotopic
777 fractionation between diatom silica and water. *Earth and Planetary Science Letters* 84: 69-74.
778 Kaufman DS, Schneider DP, McKay NP et al. (2009) Recent Warming Reverses Long-Term Arctic
779 Cooling. *Science* 325: 1236-1239.
780 Kokfelt TF, Hoernle K, Lundstrom C et al. (2009) Time-scales for magmatic differentiation at the
781 Snaefellsjokull central volcano, western Iceland: Constraints from U-Th-Pa-Ra disequilibria in post-
782 glacial lavas. *Geochimica et Cosmochimica Acta* 73: 1120-1144.
783 Kylander ME, Lind EM, Wastegård S et al. (2012) Recommendations for using XRF core scanning as a
784 tool in tephrochronology. *The Holocene* 22: 371-375.
785 Lang B, Bedford AP, Richardson N et al. (2003) The use of ultra-sound in the preparation of
786 carbonate and clay sediments for chironomid analysis. *Journal of Paleolimnology* 30: 451-460.
787 Langdon PG, Holmes N and Caseldine CJ (2008) Environmental controls on modern chironomid
788 faunas from NW Iceland and implications for reconstructing climate change. *Journal of*
789 *Paleolimnology* 40: 273-293
790 Langdon PG, Leng MJ, Holmes N et al. (2010) Lacustrine evidence of early-Holocene environmental
791 changes in northern Iceland: a multiproxy palaeoecology and stable isotope study. *The Holocene* 20:
792 205-214.
793 Langdon PG, Caseldine CJ, Croudace IW et al. (2011) A chironomid-based reconstruction of summer
794 temperatures in NW Iceland since AD 1650. *Quaternary Research* 75: 451-460.
795 Larsen G, Newton A, Dugmore A et al. (2001) Geochemistry, dispersal, volumes and chronology of
796 Holocene silicic tephra layers from the Katla volcanic system, Iceland. *Journal of Quaternary Science*
797 16: 119-132.
798 Larsen G, Eiríksson J, Knudsen K et al. (2002) Correlation of Late Holocene terrestrial and marine
799 tephra markers, north Iceland: implications for reservoir age changes. *Polar Research* 21: 283-290.

800 Larsen G and Eiríksson J (2008) Late Quaternary terrestrial tephrochronology of Iceland – frequency
801 of explosive eruptions, type and volume of tephra deposits. *Journal of Quaternary Science* 23: 109-
802 120.
803 Larsen G, Eiríksson J and Gudmundsdóttir ER (2014) Last millennium dispersal of air-fall tephra and
804 ocean-rafted pumice towards the north Icelandic shelf and the Nordic seas. In Austin WEN, Abbott
805 PM, Davies SM et al. (eds) *Marine tephrochronology*. Geological Society of London, Special
806 Publications 398: 113-140
807 Larsen DJ, Miller GH, Geirsdóttir Á et al. (2011) A 3000-year varved record of glacier activity and
808 climate change from the proglacial lake Hvítárvatn, Iceland. *Quaternary Science Reviews* 30: 2715-
809 2731.
810 Larsen DJ, Miller GH, Geirsdóttir Á et al. (2012) Non-linear Holocene climate evolution in the North
811 Atlantic: a high-resolution, multi-proxy record of glacier activity and environmental change from
812 Hvítárvatn, central Iceland. *Quaternary Science Reviews* 39: 14-25.
813 Lawson IT, Gathorne-Hardy FJ, Church MJ et al. (2007) Environmental impacts of the Norse
814 settlement: palaeoenvironmental data from Myvatnssveit, northern Iceland. *Boreas* 36: 1-19.
815 Leng MJ and Marshall JD (2004) Palaeoclimate interpretation of stable isotope data from lake
816 sediment archives. *Quaternary Science Reviews* 23: 811-831.
817 Leng MJ and Sloane HJ (2008) Combined oxygen and silicon isotope analysis of biogenic silica.
818 *Journal of Quaternary Science* 23: 313-319.
819 Liu X, Colman SM, Brown ET et al. (2013) Estimation of carbonate, total organic carbon, and biogenic
820 silica content by FTIR and XRF techniques in lacustrine sediments. *Journal of Paleolimnology* 50: 387-
821 398.
822 Massé G, Rowland SJ, Sicre M-A et al. (2008) Abrupt climate changes for Iceland during the last
823 millennium: evidence from high resolution sea ice reconstructions. *Earth and Planetary Science*
824 *Letters* 269: 565-569.
825 McGovern TH, Vésteinsson O, Friðriksson A et al. (2007) Landscapes of settlement in northern
826 Iceland: historical ecology of human impact and climate fluctuation on the millennial scale.
827 *American Anthropologist* 109: 27-51.
828 Meyers PA and Teranes JL (2001) Sediment organic matter. In Last WM and Smol JP (eds) *Tracking*
829 *environmental change using lake sediments. Volume 2: physical and geochemical techniques*. Kluwer
830 Academic Publishers, pp. 239–69.
831 Miller GH, Geirsdóttir Á, Zhong Y et al. (2012) Abrupt onset of the Little Ice Age triggered by
832 volcanism and sustained by sea-ice /ocean feedbacks. *Geophysical Research Letters* 39: L02708.

833 Morley DW, Leng MJ, Mackay AW et al. (2004) Cleaning of lake sediment samples for diatom oxygen
834 isotope analysis. *Journal of Paleolimnology* 31: 391-401.
835 Ólafsdóttir S, Jennings AE, Geirsdóttir Á et al. (2010) Holocene variability of the North Atlantic
836 Irminger Current on the south- and northwest shelf of Iceland. *Marine Micropaleontology* 77: 101-
837 118.
838 Ólafsdóttir S, Geirsdóttir Á, Miller GH et al. (2013) Synchronizing Holocene lacustrine and marine
839 sediment records using paleomagnetic secular variation. *Geology* 41: 535-538.
840 PAGES 2k Consortium (2013) Continental-scale temperature variability during the past two
841 millennia. *Nature Geoscience* 6: 339-346.
842 Pilcher JR, Hall VA and McCormac FG (1996) An outline tephrochronology for the Holocene of the
843 north of Ireland. *Journal of Quaternary Science* 11: 485–494.
844 Rieradevall M and Brooks SJ (2001) An identification guide to subfossil Tanypodinae larvae (Insecta:
845 Diptera: Chironomidae) based on cephalic setation. *Journal of Paleolimnology* 25: 81-99.
846 Rosqvist GC, Leng MJ, Goslar T et al. (2013) Shifts in precipitation during the last millennium in
847 northern Scandinavia from lacustrine isotope records. *Quaternary Science Reviews* 66: 22-34.
848 Schillereff DN, Chiverrell RC, Macdonald N et al. (2014) Flood stratigraphies in lake sediments: A
849 review. *Earth-Science Reviews* 135: 17-37.
850 Schmid PE (1993) A key to the larval Chironomidae and their instars from Austrian Danube region
851 streams and rivers. Part 1: Diamesinae, Prodiamesinae and Orthocladiinae. *Wasser und Abwasser*
852 *Supplementband* 3/93: 1-513.
853 Sicre M-A, Hall IR, Mignot J et al. (2011) Sea surface temperature variability in the subpolar Atlantic
854 over the last two millennia. *Paleooceanography* 26: PA4218.
855 Simpson I, Gudmundsson G, Thomson AM et al. (2004) Assessing the role of winter grazing in historic
856 land degradation, Myvatnssveit, northeast Iceland. *Geoarchaeology* 19: 471-502.
857 St. Amour NA, Hammarlund D, Edwards TWD et al. (2010) New insights into Holocene atmospheric
858 circulation dynamics in central Scandinavia inferred from oxygen-isotope records of lake-sediment
859 cellulose. *Boreas* 39: 770-782.
860 Straile D (2002) North Atlantic Oscillation synchronizes food-web interactions in central European
861 Lakes. *Proceedings of the Royal Society of London, Series B* 269: 391-395.
862 Striberger J, Björck S, Holmgren S et al. (2012) The sediments of Lake Lögurinn – A unique proxy
863 record of Holocene glacial meltwater variability in eastern Iceland. *Quaternary Science Reviews* 38:
864 76-88.

ter Braak CJF and Šmilauer P (2002) *CANOCO Reference Manual and CanoDraw for Windows User's Guide: Software for Canonical Community Ordination (version 4.5)*. Microcomputer Power, New York.

Thorarinsson, S. (1967) The eruptions of Hekla in historical times. The eruption of Hekla 1947-1948. Volume 1. *Societas Scientiarum Islandica*: 1-183.

Thordarsson T and Höskuldsson Á (2008) Postglacial volcanism on Iceland. *Jökull* 58: 197-228.

Trouet V, Esper J, Graham NE et al. (2009) Persistent positive North Atlantic oscillation mode dominated the Medieval Climate Anomaly. *Science* 324: 78-80.

Turney CSM (1998) Extraction of rhyolitic component of Vedde microtephra from minerogenic lake sediments. *Journal of Paleolimnology* 19: 199-206.

Velle G, Brodersen KP, Birks HJB et al. (2010) Midges as quantitative temperature indicator species: Lessons for palaeoecology. *The Holocene* 20: 989-1002.

Wiederholm T (ed) (1983) Chironomidae of the Holarctic region. Keys and diagnoses. Part I. Larvae. *Entomologica Scandinavica Supplement* 19: 1-457.

List of Figures

Figure 1: Location map of Baulárvallavatn (1a) and bathymetry, showing the coring location (1b).

Figure 2: X-radiograph and Itrax data. All elemental data are divided by the counts (kcps) and the relative smoothing of the data are shown. The geochemical data do not reveal any clear variations that can be linked to climate effects owing to the largely monolithic composition of catchment material (weathered basalt). They are successful, however, in identifying likely ash horizons, as shown by changes in the X-radiograph and associated oscillations in associated elements. Note the large spikes in K towards the base of the sequence, which represent the Landnám and Sn-1 tephras (see Table 2).

Figure 3: (a) Landnam vs SN-1 tephra plots; (b) Baulárvallavatn 23-24 cm (Hekla geochemistry) vs Hekla 1510 and Loch Portain B.

Figure 4: Chronological model produced in Bchron. Coring date, ^{137}Cs (1963) date and tephra dates (Table 2) were input. The plot shows the mean chronology and the 95% confidence limits (grey shaded areas).

Figure 5: Sedimentological and isotope data. a) sediment %TOC; b) sediment δ^{13}C; c) sediment C/N; d) low frequency magnetic susceptibility; e) frequency dependent susceptibility; f) diatom δ^{18}O.

Figure 6: Modern day isotopic composition of Baulárvallavatn and nearby lakes. The black filled circles represent a range of samples taken in April/May 2007 (end of winter) from lakes on the Snæfellsnes peninsula. Catchment sampling locations included lake inflows and outflows, snow beds and peat water inflows. The black filled squares are lake waters from Baulárvallavatn and Svínavatn, sampled in April 2006. The open diamonds reflect lake water samples taken in July 2007 (summer), and show that while most lakes plot on or near to the GMWL, two lakes (Saurarvatn and Svínavatn) plot away from the GMWL, suggesting they can be relatively evaporative in the summer. Baulárvallavatn summer water samples plot on the GMWL.

Figure 7: Baulárvallavatn chironomid percentage data (selected taxa); Chironomid-inferred temperature reconstructions, and PCA axis 1 scores.

Figure 8: Chironomid PCA axis 1 score reconstruction. Reconstruction using mean chronology is in black. Reconstructions using 1000 sample chronologies are in grey.

Figure 9: Composite diagram, comparing the chironomid results (PCA axis 1 reconstruction and % head capsule concentration) against the organics proxies from BAUL (%TOC, $\delta^{13}C$ and C/N) and the diatom $\delta^{18}O$.

Figure 10: Composite diagram, showing chironomid results (PCA axis 1 reconstructions) against selected terrestrial and marine proxies from Iceland including Stora Viðarvatn chironomid inferred summer temperature (Axford et al. 2009), Haukadalsvatn BSi (Geirsdottir et al. 2009b), Hvítárvatn ice thickness (Larsen et al. 2011), and offshore alkenone water temperatures (Sicre et al. 2011).

Figure 11: Comparison of chironomid variability against NAO over the last 1000 years.

List of Tables

Table 1. Radiocarbon determinations from the BAUL sequence.

Table 2. Details of the tephra found in each depth layer investigated. The different volcanic centres are represented by Ka (Katla), Ve (Vei›ivötn), Gr (Grímsvötn), Sn (Snæfellsnes) To (Torfajökull) and Hk (Hekla). The numbers in parentheses after each eruption centre relate to the number of shards identified from that centre according to the major element results (see Sup. Material). The tephra in the right hand column represents the most likely eruption ascribed to each depth layer, as discussed in the text. Note, for the 14-15 cm layer, both ages are used in the generation of the age model (Figure 4).

Supplementary Material

Excel spreadsheet with detailed geochemical data from each tephra shard analysed under EMPA from the BAUL sequence.

Fig 1

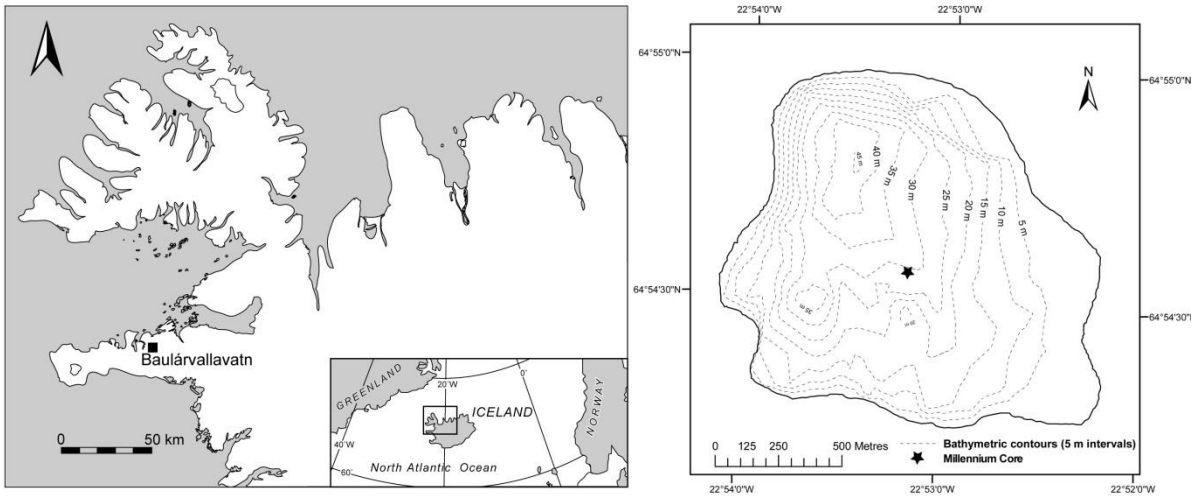
Baulárvallavatn
0
50 km
GREENLAND
ICELAND
NORWAY
North Atlantic Ocean
20°W
40°W
60°
0°
22°54'0"W
22°53'0"W
22°52'0"W
64°55'0"N
64°54'30"N
N
40 m
35 m
30 m
25 m
20 m
15 m
10 m
5 m
0 125 250 500 Metres
Bathymetric contours (5 m intervals)
Millennium Core

Fig 2

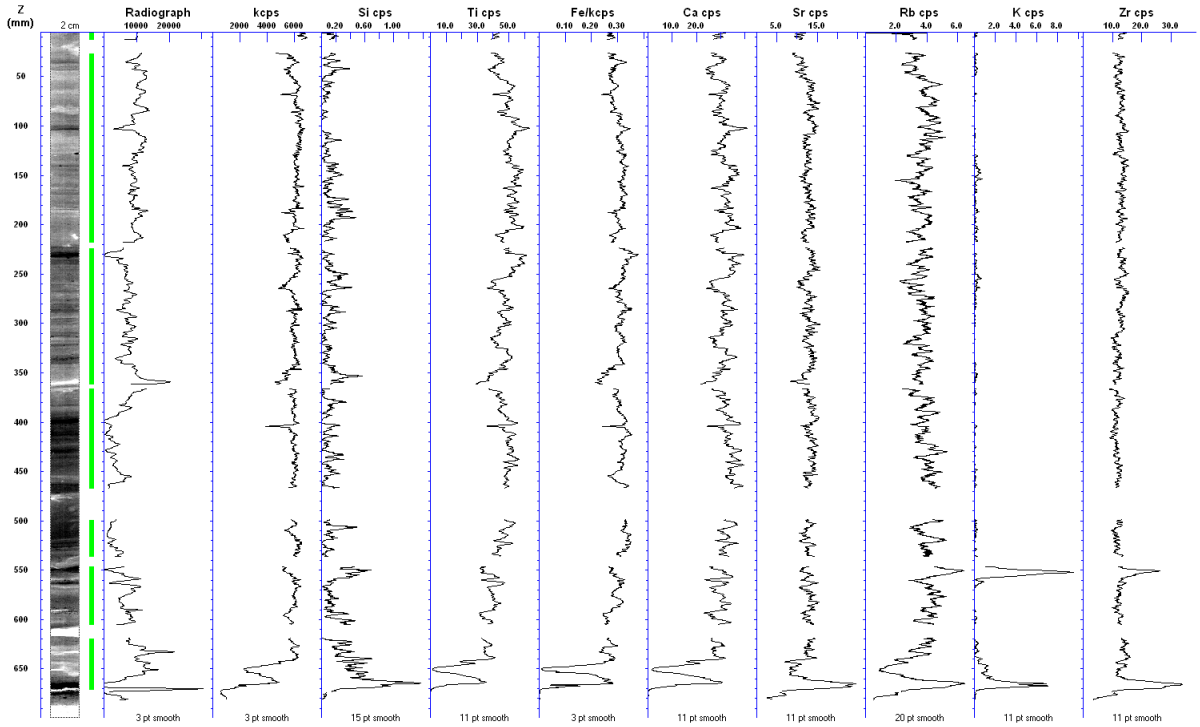

Core: BAULAR-Da	Section: 1 FILM	User: PLANGDON4	Date: 04/09/2006 - ItraX-PLOT V2.68
X-Ray tube: Mo target	Line camera signal 38717 at 25 ms	Filename: BAULAR-Da-1 FILM	Data produced by the NOC Itrax
XRF Conditions	30 kV 30 mA	Step Size: 200 microns	Count-time: 15 seconds/increment
X-radiograph Conditions	45 kV 40 mA	Step Size: 200 microns	Dwell time: 400 ms/increment

Fig 3

FIG X

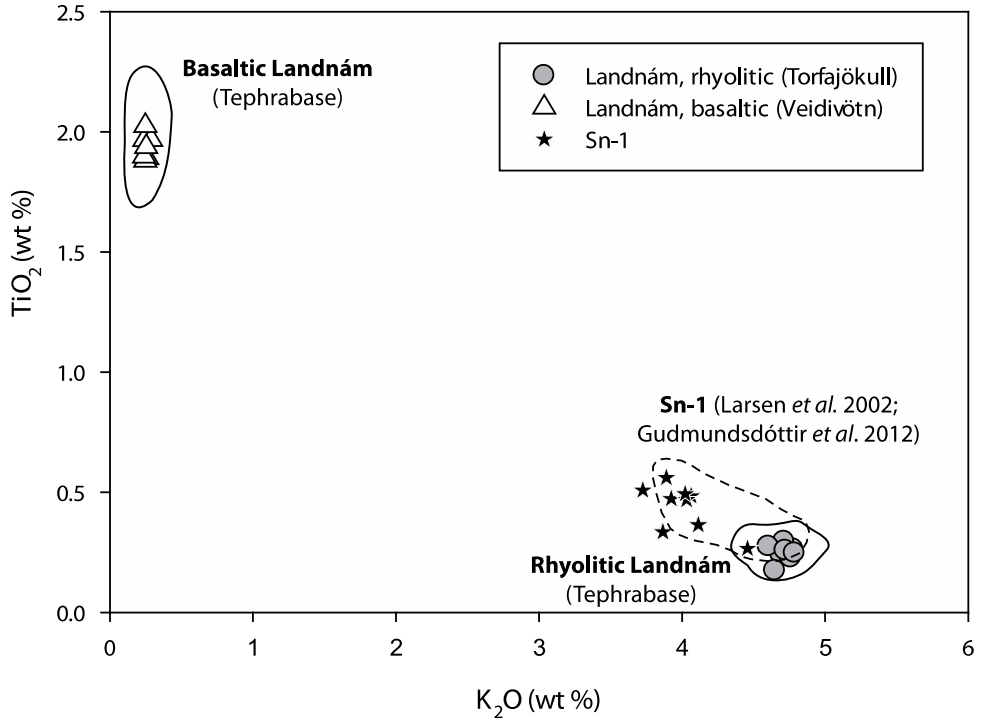

FIG Y

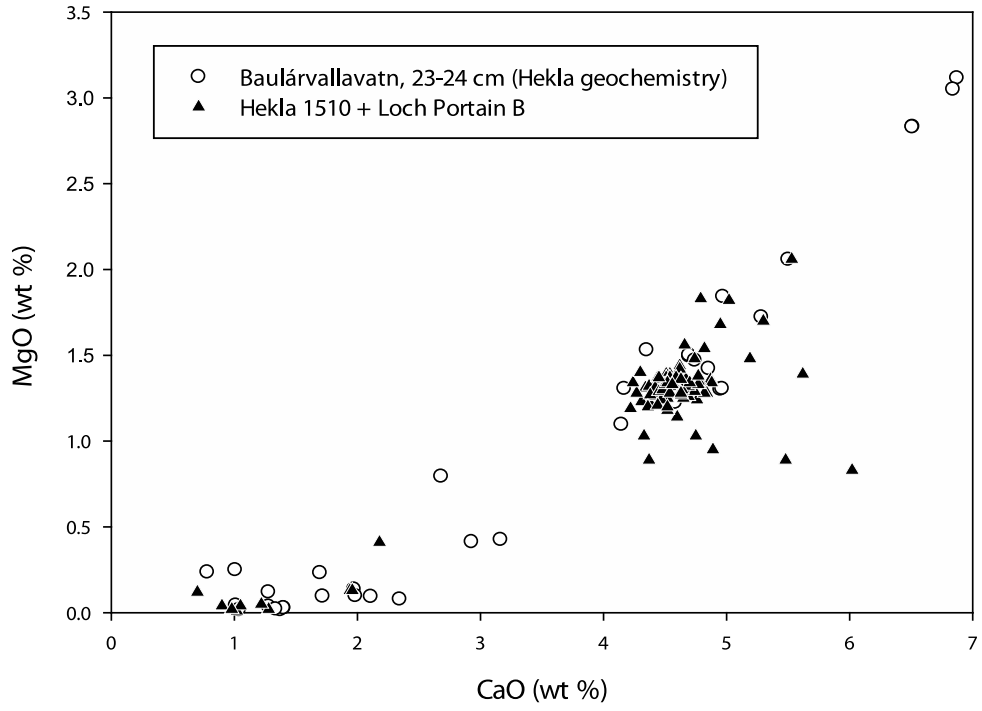

Fig 4

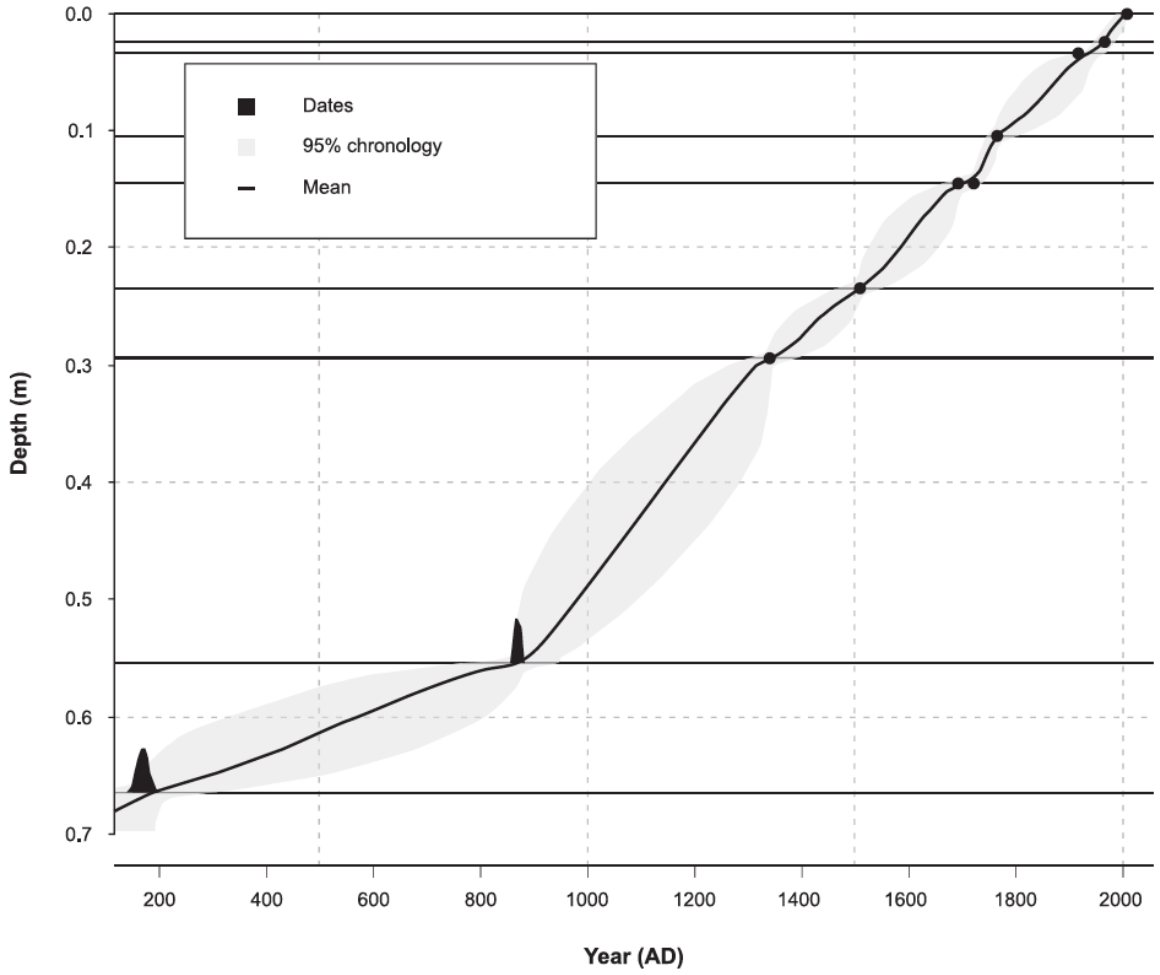
Dates
95% chronology
Mean
Depth (m)
0.0
0.1
0.2
0.3
0.4
0.5
0.6
0.7
200
400
600
800
1000
1200
1400
1600
1800
2000
Year (AD)

Fig 5

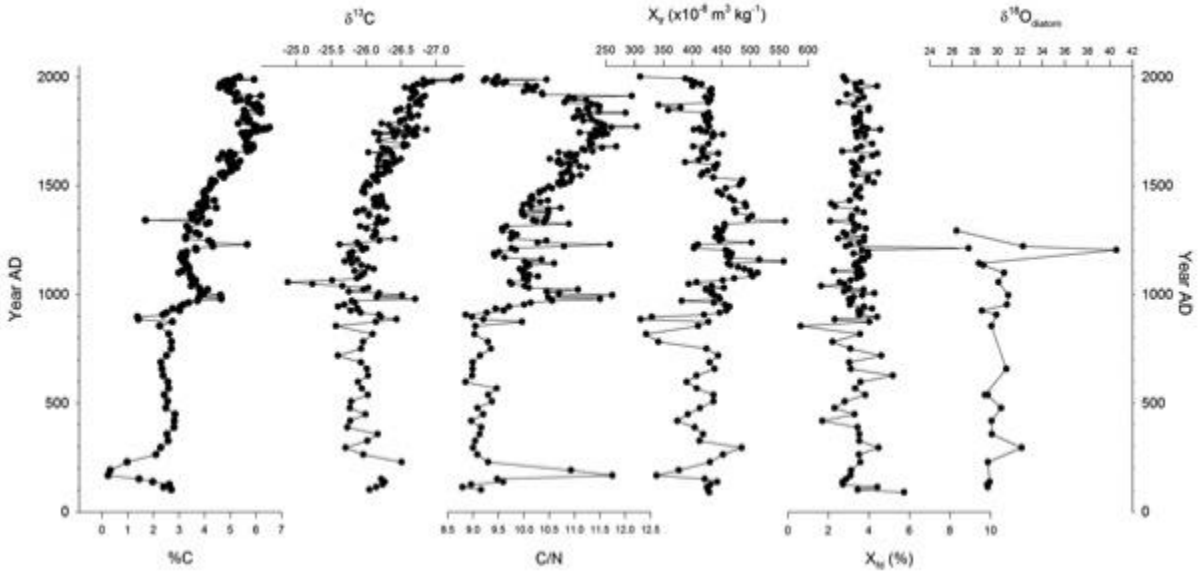

Fig 6

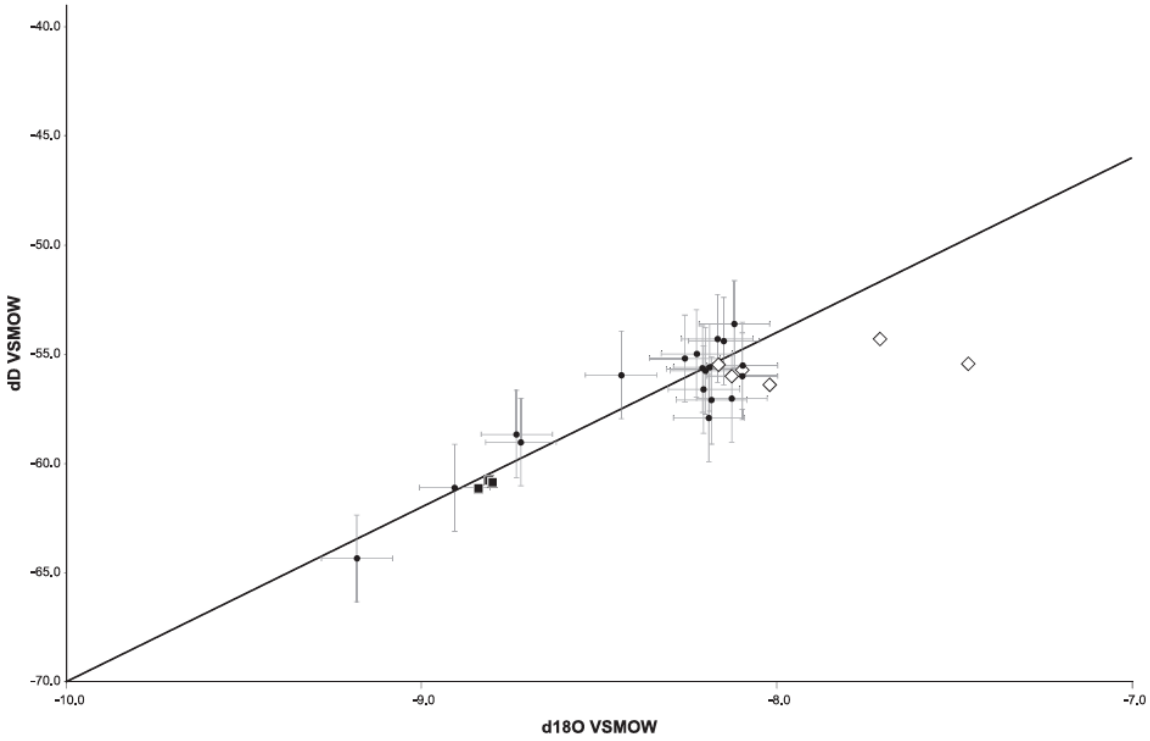

Fig 7

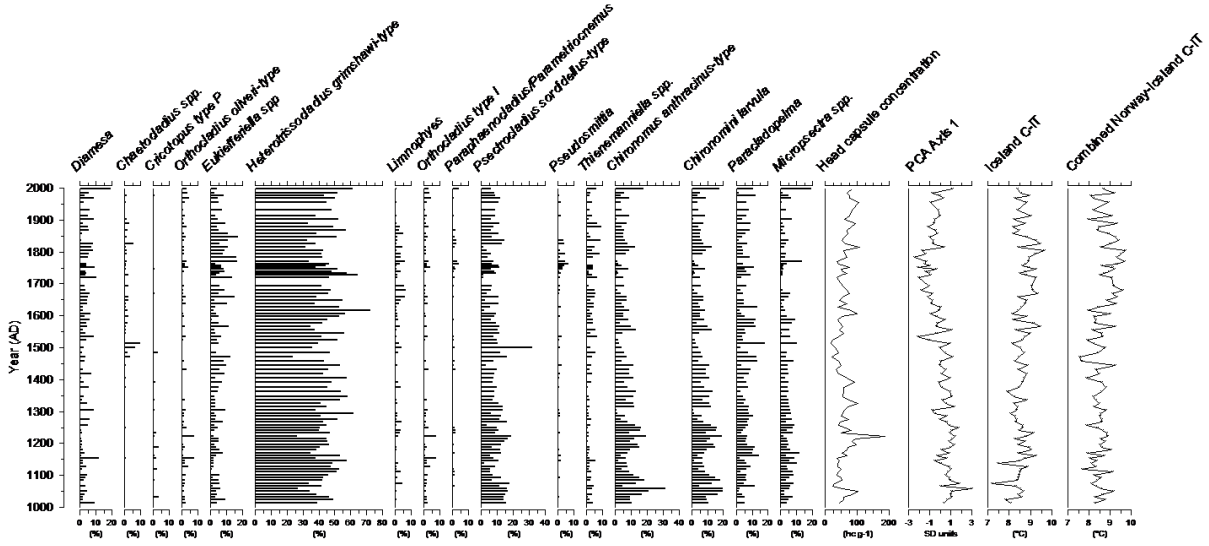
Diamesa
Chaetocladius spp.
Cricotopus type P
Orthocladius oliveri-type
Eukiefferiella spp
Heterotrissocladius grimshawi-type
Limnophyes
Orthocladius type I
Paraphaenocladius/Paramerionemus
Psectrocladius sordidellus-type
Pseudosmittia
Thienemanniella spp.
Chironomus anthracinus-type
Chironomini larvula
Paracladopelma
Micropsectra spp.
Head capsule concentration
PCA Axis 1
Iceland C-IT
Combined Norway-Iceland C-IT
Year (AD)
2000
1900
1800
1700
1600
1500
1400
1300
1200
1100
1000
(%)
(hc g-1)
SD units
(°C)

Fig 8

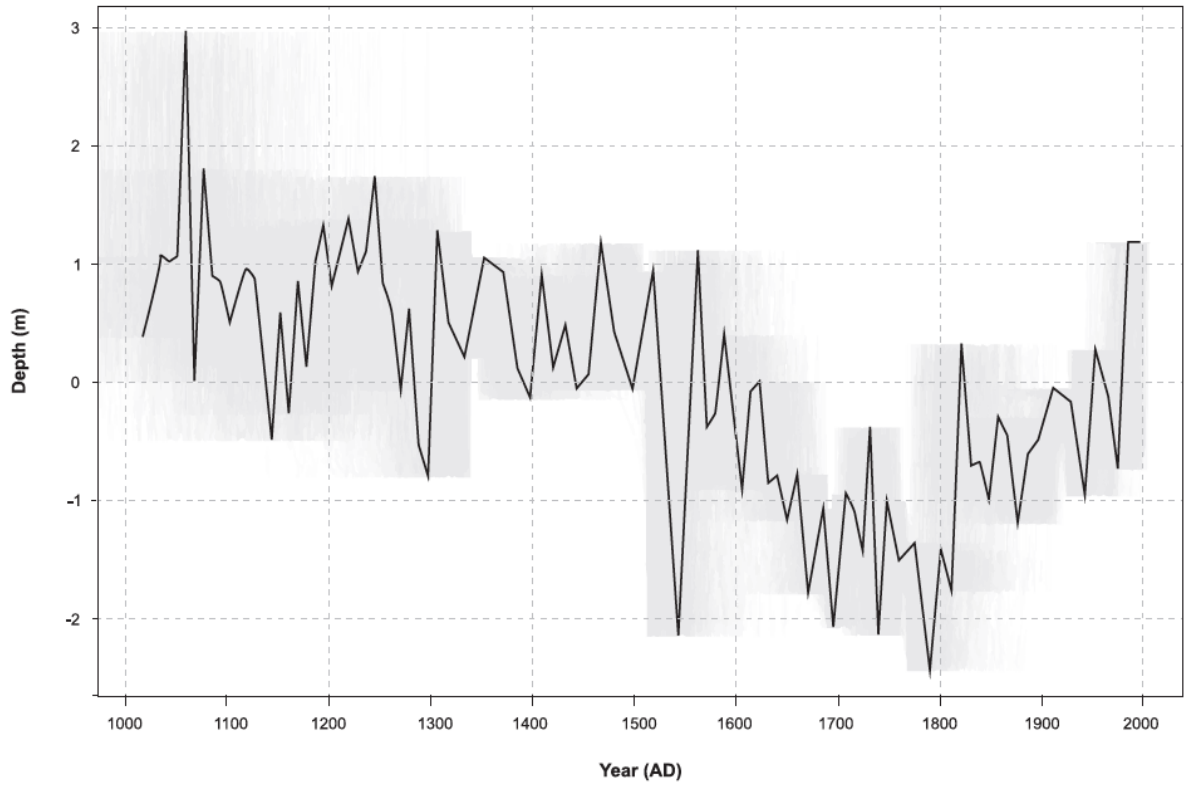
Depth (m)
3
2
1
0
-1
-2
1000
1100
1200
1300
1400
1500
1600
1700
1800
1900
2000
Year (AD)

Fig 9

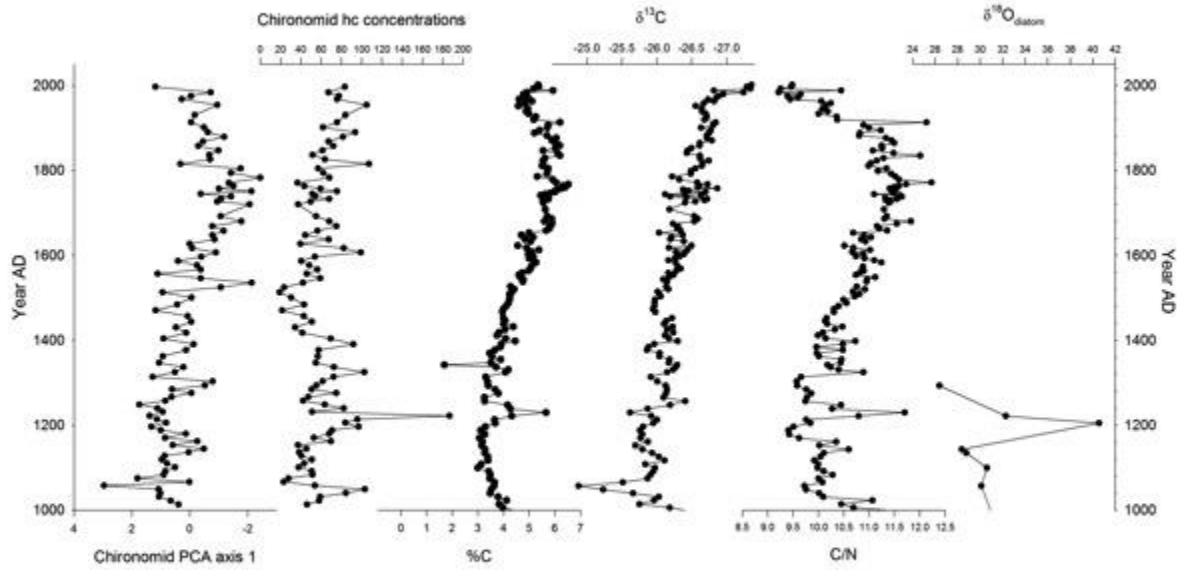
Chironomid hc concentrations
δ13C
δ18Odiatom
Year AD
Chironomid PCA axis 1
%C
C/N

Fig 10

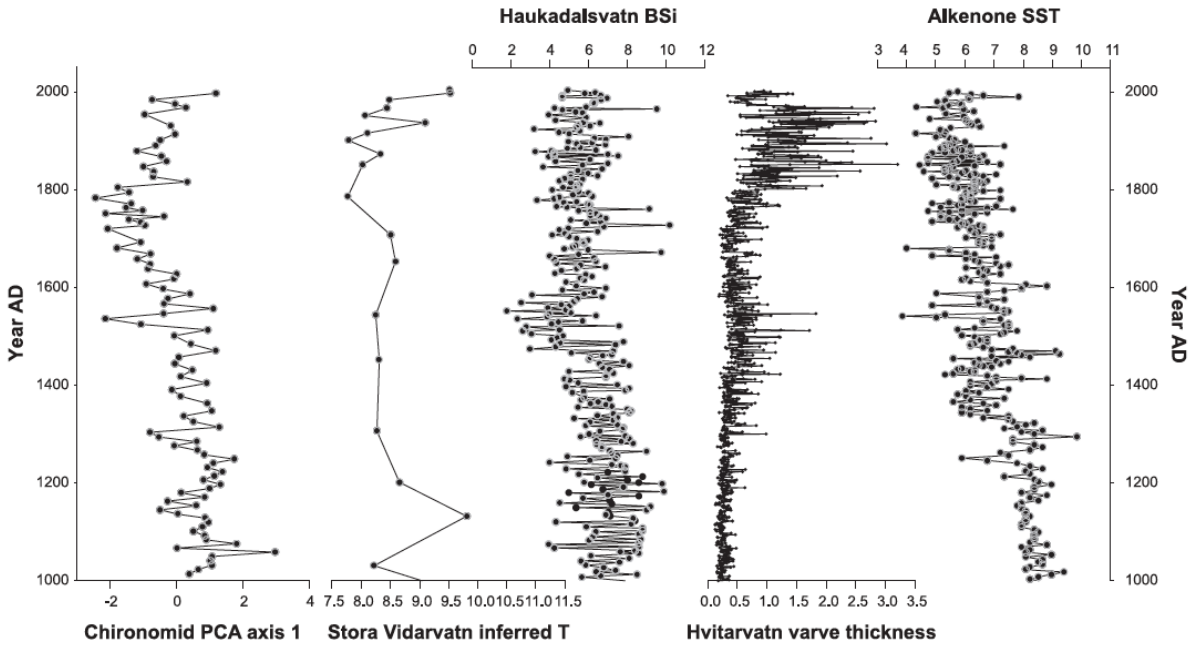
Haukadalsvatn BSi
Alkenone SST
Year AD
2000
1800
1600
1400
1200
1000
-2 0 2 4
Chironomid PCA axis 1
7.5 8.0 8.5 9.0 9.5 10.0 10.5 11.0 11.5
Stora Vidarvatn inferred T
0.0 0.5 1.0 1.5 2.0 2.5 3.0 3.5
Hvitarvatn varve thickness
0 2 4 6 8 10 12
3 4 5 6 7 8 9 10 11

Fig 11

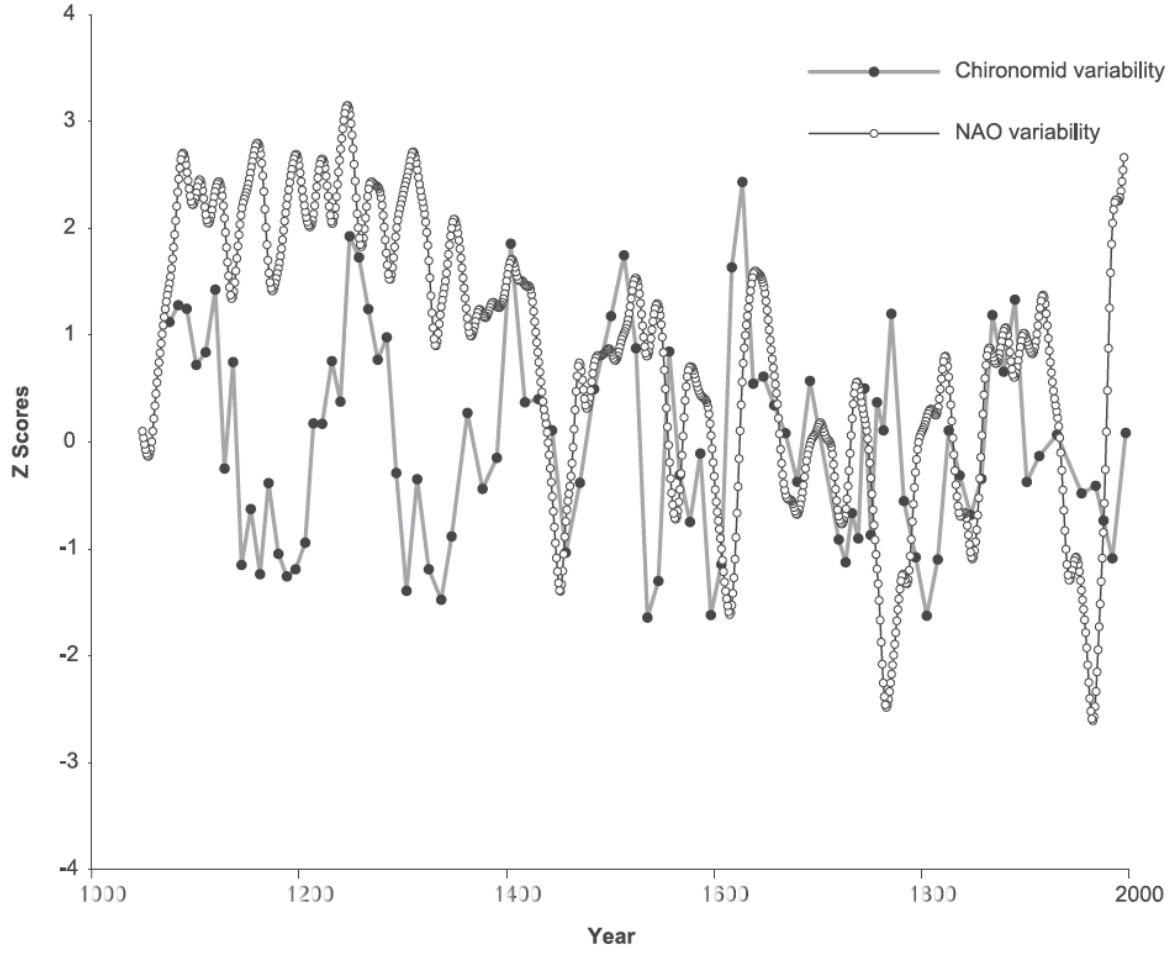
Chironomid variability
NAO variability
Z Scores
Year
4
3
2
1
0
-1
-2
-3
-4
1000
1200
1400
1600
1800
2000